800545

HANDLING-CHARACTERISTICS SIMULATIONS OF CAR-TRAILER SYSTEMS

R. J. Anderson, Defence Research Establishment Atlantic
(Dartmouth/Nova Scotia)

E. F. Kurtz, Jr., Dept. of Mechanical Engrg.
Queen's Univ.
(Kingston/Ontario)

ABSTRACT

Two theoretical models are described for simulating the handling characteristics of automobiles towing trailers. These models are similar except that one excludes roll dynamically and has only four degrees of freedom, whereas the other includes roll dynamically and has six degrees of freedom. Both models are extensively validated by comparing digital-computer results obtained from them with experimental data obtained by Systems Technology, Inc. Both models yielded excellent simulations of measures of handling characteristics, the model with six degrees of freedom being slightly superior. Nonetheless, the most important conclusion of this study is that excellent simulations of handling characteristics of car-trailer systems can be obtained with a model having only four degrees of freedom. The study includes a sensitivity analysis to indicate the importance of certain effects included in the models.

THE PRIMARY OBJECTIVES OF THE WORK reported here were to develop simple theoretical models useful for investigating the dynamic behavior of automobiles towing trailers, and to validate these models using experimental data for real car-trailer systems. The measure of simplicity was the number of degrees of freedom in the model, and not necessarily the complexity of the interactions between the system elements and the environment.

Our work focussed on one of the many aspects of dynamic behavior, namely handling characteristics — lateral motions of the vehicle system. The models described here deal with the response of the vehicle system to prescribed steering inputs at the front wheels of the towing vehicle, with the vehicle system travelling at approximately constant forward velocity.

The timing of this project turned out to be fortunate, because it happened that Systems Technology Inc. (STI) completed an extensive experimental investigation of automobiles towing trailers [2, 10, 25, 26, 27] * just as our model-development work was approaching completion, producing data ideally suited for validating our models.

Our modelling efforts drew extensively from the efforts of others. We recently published a review of the state-of-the-art as regards automobiles towing trailers [11]. We shall mention here only those works from which we directly drew guidance and material. We referred extensively to the book by Ellis [7] in which he also specifically considers automobile-trailer systems. In fact, one of our models is very similar to a model reported by Ellis. Perhaps the most critical element of the models we developed is the method for representing tire forces. Here we employed tire-force data produced by Calspan Corp. [3, 5, 13, 15 – 24]; specifically, we employed an empirical mathematical representation of these data as presented by Bohn and Keenan [4].

In this paper we shall only summarize the most important aspects of our car-trailer models and their validation. Anderson has presented a detailed description of the models in his Ph.D. Thesis [1].

MODEL DESCRIPTIONS

Two models were developed for representing the lateral dynamics of automobiles towing trailers, one with four degrees of freedom (4DOF), and one with six degrees of freedom (6DOF). The intent behind developing these two models was to make a comparison of them as part of a sensitivity analysis to determine the importance of certain effects.

The four-degree-of-freedom model (4DOF) is illustrated in Fig. 1. The degrees of freedom used in this model are those used by Ellis [7]. The center of mass of the car body has longitudinal motion at velocity U, lateral motion at velocity V, and yawing motion at a yaw rate r. The trailer has an articulated angle ψ. Both front wheels of the towing vehicle have an identical prescribed steer angle δ_F.

Our model incorporates some effects not in the model described by Ellis [7]. The tire-force model is completely different. Lateral tire flexibility was taken into account as will be described in the section on tire forces. Aerodynamic lift and drag forces on the car and trailer bodies were included. Steering angles δ_R at the rear axle of the car and δ_T at the axle of the trailer due to roll of the car and trailer bodies were accounted for approximately by assuming that roll motions of the car and trailer bodies could be determined by static-equilibrium requirements, and that steer angles of these axles could also then be determined by roll-steer compliances effects. Coefficients relating the body roll angles to static-equilibrium lateral forces applied at the centers of mass of the car and trailer bodies were estimated (body roll angle per

*Numbers in brackets designate References at the end of paper.

SAE/SP-80/463/$02.50

unit lateral force). The coefficients for body roll angle per unit lateral force were combined with the axle roll-steer compliance coefficients (steer angle per unit body roll angle) to yield to roll-steer coefficients (axle-steer angle per unit lateral force) for forces at the car and trailer centers of mass. Lateral inertia forces at these centers of mass were thus used to estimate the wheel-assembly steer angles.

The tire forces in 4DOF were modelled neglecting the effects of load transfer from one side of the vehicle to the other due to lateral accelerations, and this resulted in the estimation of these tire forces on the basis of loads per axle. A possible future refinement would be to treat all the tires in 4DOF individually and model the normal tire loads on a quasi-static basis as was done in treating the roll.

The six-degree-of-freedom model (6DOF) is illustrated in Fig. 2. The degrees of freedom used here are the same as those used for 4DOF with the addition of roll degrees of freedom, ϕ_C, for the car body and, ϕ_T, for the trailer body. As for 4DOF, both front wheels of the car in 6DOF are assumed to have an identical prescribed steer angle δ_F. The roll of the car and trailer bodies was defined as rotation about longitudinal axes through the centers of mass. These centers of mass are slightly different from the corresponding centers for 4DOF, because the bodies in 6DOF do not include the wheel-axle assemblies whereas those for 4DOF include them. The wheel-axle assemblies in 6DOF have translational and yaw motions, but do not have any roll motions. The steering angles, δ_R, of the rear axle of the car and, δ_T, of the trailer axle in 6DOF were accounted for by using the axle roll-steer compliances and computing the body roll dynamically. Tire forces were modelled for 6DOF in the same fashion as in 4DOF with the exception that all tires were considered individually in 6DOF, including the effects of individual tire normal loads on the tire forces. Aerodynamic forces were taken into account in 6DOF exactly as they were in 4DOF.

The methods for modelling roll in the four- and six-degree-of-freedom models are similar. The roll model is illustrated in Fig. 3 which shows the body (for either the car or the trailer) rolled through an angle ϕ about a longitudinal axis. Rotation about an axis passing through the center of mass, with no other lateral motion of the body center of mass, results in a lateral motion $H\sin\phi$ of the wheel assemblies. Each wheel-assembly motion was assumed to be tangential to the ground, and was determined by employing the roll-center concept as shown in Fig 3. The actual wheel-assembly motion depends on the motion of the complete vehicle system as governed by the forces exerted on this system.

The roll-center approach described above for modelling the roll-dynamics is recognized as being approximate. One inconsistency arises immediately in this regard; when the roll-center locations of the front and rear axle assemblies differ, as they generally do, there should be some body yaw associated with the body roll. No attempt was made in this work to account for this yaw effect, because it was expected that the effects of body roll on the lateral dynamics were indirect and small, being primarily due to roll-steer effects. This expectation was supported by the results obtained with the model.

The experimental data used to validate the theoretical models described here included tests with a load-transfer device as shown in Fig. 4. Such a device causes a redistribution of the normal loads on the tires, and more importantly, the device tested exerts a restoring torque at the trailer hitch opposing articulation. Our model for this device is discussed in the Load-Transfer Device Section.

TIRE-FORCE MODELS

The models for the forces exerted on the car-trailer system by the tires were perhaps the most critical part of the modelling process. We shall thus discuss the tire models in some detail.

Two distinct aspects of the tire forces were taken into account. The first concerns the steady-state values of the lateral tire forces, and how these lateral tire forces depend on the slip between the tire and the road and other factors. The second aspect concerns the effects of lateral flexibility in the tire sidewall, and the consequent transient behavior of lateral tire forces.

Our steady-state, tire-force model was that developed by the Calspan Corp. [3, 5, 13, 15 – 24] as described by Bohn and Keenan [4] of Johns Hopkins Univ. The equations for this model are presented below. Fig. 6 illustrates the definitions of the steady-state tire-force variables.

The steady-state lateral tire force Y is described by the relation

$$Y = -\mu_y Z\, g(\bar{\theta})\, F(S) \tag{1}$$

where:

μ_y = coefficient of friction for lateral sliding of the tire
Z = normal force exerted on the tire by the road
$g(\bar{\theta})$ = dimensionless side-slip function
$F(S)$ = dimensionless longitudinal-slip function

The friction coefficient μ_y is given by

$$\mu_y = (B_1 Z + B_2 \left[U_w^2 + V_w^2\right] + B_3 + B_4 Z^2)\, SN \tag{2}$$

where:

B_i = constants depending on tire characteristics
SN = ratio of skid number of the road surface to skid number of test surface for which the B_i are appropriate
U_W, V_W = longitudinal and lateral components of the wheel-center velocity

The function $g(\bar{\theta})$ in Eq. (1) was selected on an ad-hoc basis because it has an appropriate shape for describing tire behavior, and is

$$g(\bar{\theta}) = \begin{cases} \bar{\theta} - \bar{\theta}|\bar{\theta}|/3 + \bar{\theta}^3/27 \text{ if } |\bar{\theta}|<3 \\ \bar{\theta}/|\bar{\theta}| \text{ if } |\bar{\theta}|\geq 3 \end{cases} \tag{3}$$

Note that $g(3) = 1$ with $g'(3)$ and $g''(3) = 0$. The argument $\bar{\theta}$ is a measure of the side-slip angle of the tire contact patch and is defined as follows:

$$\bar{\theta} = \frac{A_1 \nu(\nu - A_2) - A_o A_2}{A_2 \mu_y Z}(\theta + \theta') \tag{4}$$

where:

θ = the tire contact-patch slip angle

The steering effect θ' due to wheel camber γ is taken into account using

$$\theta' = \frac{A_2 A_3 (A_4 - \nu)\nu}{A_4 [A_1 \nu (\nu - A_2) - A_o A_2]} \gamma$$

$$\gamma = -K_w Y \tag{5}$$

$$\nu = \begin{cases} Z \text{ if } Z \leq \eta A_2 \\ \eta A_2 \text{ if } Z > \eta A_2 \end{cases}$$

where:

A_i = constants for representing tire behavior

η = a constant for representing tire behavior

We accounted in Eq. (5) only for the deviation in wheel camber, this deviation γ being a compliance effect assumed proportional, via K_w, to the lateral force Y.

The function F(S) in Eq. (1) is used to account for the fact that lateral tire forces are reduced by the effects of longitudinal tire slip, S, itself a function of the longitudinal tire force X. The values of longitudinal tire force were always sufficiently small to permit F(S) to be taken as unity with less than 1% error for all this work. Consequently the tire lateral-force relation Eq. (1) is primarily a function only of the side-slip angle θ:

$$Y = Y(\theta) \tag{6}$$

If this work were to be extended to take large traction or braking forces into account, it would be appropriate to reassess the evaluation of F(S).

The form of Eq. (1) suggests that the lateral force Y is proportional to the friction coefficient μ_Y. We will show below that Y is actually independent of μ_Y for sufficiently small values of the tire side-slip parameter $\bar{\theta}$.

From Eq. (3), for small values of $\bar{\theta}$

$$g(\bar{\theta}) \approx \bar{\theta} \tag{7}$$

so that, from Eq. (1) and Eq. (4) and assuming F(S) = 1,

$$Y \approx -\frac{A_1 \nu (\nu - A_2) - A_o A_2}{A_2} (\theta + \theta') \tag{8}$$

This is independent of sliding-friction effects.

The tire aligning torque T in Fig. 5 accounts for the fact that the resultant lateral tire force does not act through the center of the contact patch. We again used the Calspan model [3, 5, 13, 15 – 24]; i.e.

$$T = (C_1 Z + C_2 |Y|) Y + C_3 Z \gamma \tag{9}$$

where:

C_i = constants for representing tire behavior

Our model for taking into account the effects of lateral tire flexibility is based on the concept that a lateral tire force will cause a corresponding lateral displacement of the contact patch relative to the wheel center. If this lateral force is changing with time, so also will this lateral displacement change with time, thus making the slip angle of the contact patch different from that of the wheel center. This situation differs from the steady-state situation in which the slip angle of the contact patch equals that of the wheel center. Essential to our model is the assumption that the instantaneous relation between the lateral tire force and the contact-patch slip angle is the same for both the steady-state and the transient situations.

Our model for taking into account the effects of lateral tire flexibility is illustrated in Fig. 7. If a lateral force Y is exerted on the tire contact patch, this contact patch will be displaced an amount y_c such that

$$Y = K_\ell y_c \tag{10}$$

where:

K_ℓ = tire side-wall stiffness (approximately half the vertical tire stiffness)

y_c = lateral displacement of the contact patch

If the contact-patch displacement is changing with time, there is the geometric requirement that

$$\tan\theta = (V_w + \dot{y}_c)/U_w \tag{11}$$

where:

θ = side-slip angle of the contact patch

We distinguish now between the slip-angle θ of the contact patch and the slip angle α of the wheel center. For the latter,

$$\tan\alpha = V_w/U_w \tag{12}$$

Combining Eq. (11) and Eq. (12) yields

$$\dot{y}_c = U_w(\tan\theta - \tan\alpha) \tag{13}$$

To proceed further we assume that the lateral force Y in Eq. (10) is a function Eq. (6) of the side-slip angle θ, and that this function is identical to the steady-state relation between Y and the side-slip angle. Implicit, here, is the assumption that inertia-force effects within the tire side wall are negligible. Thus from Eq. (10)

$$Y(\theta) = K_\ell y_c \tag{14}$$

Differentiating this with respect to time

$$\dot{y}_c = \frac{1}{K_\ell} \frac{dY}{d\theta} \dot{\theta} \tag{15}$$

where $dY/d\theta$ is the local slope of the $Y(\theta)$ function. Combining Eq. (13) and Eq. (15)

$$\dot{\theta} = K_\ell U_w (\tan\theta - \tan\alpha)/(dY/d\theta) \tag{16}$$

This simple model can yield results consistent with observed transient tire-force behavior. For example, for small values of θ and α, the response to a step function in α from $\theta = 0$ is

$$\frac{Y(x)}{Y(\infty)} = 1 - \exp[-K_\ell x/(dY/d\theta)] \tag{17}$$

where x denotes the distance rolled by the tire after the step in α occurred. It is well known [14] that tires do respond to a step steer as described by Eq. (17). For example, using typical appropriate values for K_ℓ and $dY/d\theta$, Eq. (17) predicts that transient effects disappear after the tire rolls between one and two revolutions, consistent with observed behavior.

Our's is a first-order model of transient tire behavior requiring parameter data which can be measured statically. Lippmann and Oblizajek [12] developed a second-order model which matches experimental tire data well, but relies upon transient tire-force data for evaluating the parameters used in their model. We shall show later that transient tire effects were not significant in our simulations, conclusions reached also by Lippmann and Oblizajek.

LOAD-TRANSFER DEVICE

One of the unique and perhaps most significant aspects of the work reported here concerns simulation of a load-transfer device as shown in Fig. 4. Such a device was used for certain tests performed by STI.

It is well known that a car-trailer system is made more stable as regards the flutter type of instability as the trailer center of gravity (CG) is moved forward. The intent of this load-transfer device is to transfer some of the normal load from the rear tires of the car to the trailer tires and the front wheels of the car, facilitating the use of such a forward CG without excessive tire and suspension-system loads. The design of this particular device introduces another characteristic which, it turns out, is also favorable as regards all types of car-trailer instabilities. We shall show that this device introduces a torque tending to resist trailer articulation.

The equalizer bar is mounted on a pin at its hitch end, with considerable friction in this pin. Thus, as the trailer articulates, the positions of the equalizer bars tend to remain fixed if the trailer articulation is sufficiently small. The angles which the tension chains make with respect to the trailer tongue then change to generate a lateral component of the forces exerted on the trailer tongue by these chains. These lateral-force components exert a restoring moment on the trailer hitch proportional to the deviation of the articulation angle for sufficiently small articulation angles. However, if these lateral forces become sufficiently large to overcome the friction in the equalizer-bar pins, the equalizer bars swing with the trailer, yielding an articulation torque which remains constant as long as the magnitude of the articulation angle keeps increasing.

The mathematical stick-slip friction model used for this load-transfer device is depicted in Fig. 7 and is as follows:

$$T_\psi = \begin{cases} T_{\psi 1} \text{ if } d|\psi - \psi_o|/dt > 0 \text{ and } T_{\psi 1} < \text{Max } (T_{\psi 1}) \\ T_{\psi 2}\,\text{sign } (\dot{\psi}) \text{ if } T_{\psi 1} > \text{Max } (T\psi_1) \end{cases} \quad (18)$$

where:

$T_{\psi 1} = K_\psi(\psi - \psi_o)$

$T_{\psi 2}$ = constant

where Max($T_\psi 1$) denotes the torque required to break the static-friction forces. The reference angle ψ_o changes if the equalizer bars do swing, being always the articulation angle for which the load equalizer would exert no articulation torque.

The values of Max($T_\psi 1$) and $T_\psi 2$ used in the load-equalizer model correspond to static and sliding friction-coefficient values of 0.74 and 0.57 respectively. The K_ψ value used was estimated as described by Anderson [1] from the load-equalizer geometry and measured tension-chain force.

EQUATIONS OF MOTION FOR 4DOF

We shall present below the equations of motion in some detail for our four-degree-of-freedom model, 4DOF. The derivation was performed using Lagrange's equations, and we thus automatically obtained symmetric inertia-force terms. Our equations can be rearranged to be the same as those presented by Ellis [7] with modifications due to our inclusion of aerodynamic forces, compliance effects, the load-transfer device, and the way we modelled tire forces. The variables are illustrated in Figs. 1 and 8. Our equations are

$$\begin{bmatrix} (m_C+m_T) & 0 & m_T h_2 \sin\psi & m_T h_2 \sin\psi \\ 0 & (m_C+m_T) & -m_T(h_1+h_2\cos\psi) & -m_T h_2 \cos\psi \\ m_T h_2 \sin\psi & -m_T(h_1+h_2\cos\psi) & I_{22} & I_{23} \\ m_T h_2 \sin\psi & -m_T(h_2\cos\psi) & I_{32} & I_{33} \end{bmatrix} \begin{Bmatrix} \dot{U} \\ \dot{V} \\ \dot{r} \\ \ddot{\psi} \end{Bmatrix} = \begin{Bmatrix} R_1 \\ R_2 \\ R_3 \\ R_4 \end{Bmatrix} \quad (19)$$

where:

$$I_{22} = I_C + I_T + m_T(h_1^2 + h_2^2) + 2m_T h_1 h_2 \cos\psi$$

$$I_{33} = I_T + m_T h_2^2$$

$$I_{23} = I_{33} + m_T h_1 h_2 \cos\psi; \quad I_{32} = I_{23}$$

The force functions R_i are as follows:

$$
\begin{aligned}
R_1 &= 2X_F\cos\delta_F + 2X_R\cos\delta_R + 2X_T\cos(\psi + \delta_T) \\
&- 2Y_F\sin\delta_F - 2Y_R\sin\delta_R - 2Y_T\sin(\psi + \delta_T) \\
&+ X_{AC} + X_{AT}\cos\psi - Y_{AT}\sin\psi \\
&+ (m_C + m_T)Vr - m_T h_1 r^2 - m_T h_2 (r + \dot{\psi})^2\cos\psi \\
R_2 &= 2X_F\sin\delta_F + 2X_R\sin\delta_R + 2X_T\sin(\psi + \delta_T) \\
&+ 2Y_F\cos\delta_F + 2Y_R\cos\delta_R + 2Y_T\cos(\psi + \delta_T) \\
&+ Y_{AC} + X_{AT}\sin\psi + Y_{AT}\cos\psi \\
&- (m_C + m_T)Ur - m_T h_2 (r + \dot{\psi})^2\sin\psi \\
R_3 &= 2aX_F\sin\delta_F - 2bX_R\sin\delta_R - 2h_1 X_T\sin(\psi + \delta_T) \\
&+ 2aY_F\cos\delta_F - 2bY_R\cos\delta_R - 2Y_T\left[h_2 + c + h_1\cos(\psi + \delta_T)\right] \\
&+ 2T_F + 2T_R + 2T_T \\
&- X_{AT}h_1\sin\psi - Y_{AT}(h_2 + h_1\cos\psi) + T_{AC} + T_{AT} \\
&+ m_T h_2 (V\sin\psi + U\cos\psi)r + m_T h_1 Ur + m_T h_1 h_2 (\dot{\psi}^2 + 2r\dot{\psi})\sin\psi \\
R_4 &= -2Y_T(h_2 + c) + 2T_T - Y_{AT}h_2 + T_{AT} \\
&+ m_T h_2 (U\cos\psi + V\sin\psi)r - m_T h_1 h_2 r^2\sin\psi - T_\psi
\end{aligned}
\tag{20}
$$

The tire forces are calculated using the procedures described in the Load-Transfer Device Section. We shall describe below how those procedures were applied to the model 4DOF. For this four-degree-of-freedom model, it is possible to represent the tire-force reactions on all the tires on any specific axle by a resultant force and a resultant couple, the centroid of the force reaction being at the axle center. We used this model for 4DOF as shown in Fig. 8, where we show the force and torque resultants as 2Y and 2T respectively since our vehicles had two tires on each axle, and X, Y, and T denote force reactions on a single tire. These tire-force reactions are to be calculated in terms of an average slip angle which would be experienced by a ficticious tire at the tire-force centroid for the axle. The longitudinal tire-force reactions X at each axle are treated as independent variables for the simulation. The wheel-center slip angles used for calculating the lateral forces are as follows:

$$
\begin{aligned}
\alpha_F &= \delta_F - \text{atan}\,(V + ra)/U \\
\alpha_F &= \delta_F - \text{atan}\,(V - rb)/U \\
\alpha_T &= \delta_T - \text{atan}\{[(V - rh_1)\cos\psi - U\sin\psi - (h_2 + c)(r + \dot{\psi})] \\
&\qquad /[U\cos\psi + (V - rh_1)\sin\psi]\}
\end{aligned}
\tag{21}
$$

The front-axle steering angle, δ_F, is a prescribed function. The other steer angles δ_R and δ_T are due to roll-steer; i.e.

$$
\begin{aligned}
\delta_R &= C_R m_C(\dot{V} + rU) \\
\delta_T &= C_T m_T\left[(\dot{V} + rU - h_1\dot{r})\cos\psi - h_2(\dot{r} + \ddot{\psi}) - (\dot{U} + h_1 r^2)\sin\psi\right]
\end{aligned}
\tag{22}
$$

The roll-steer compliances C_R and C_T are found using Eq. (28) as described below.

The slip-angle relations Eq. (21) are used to calculate the values of α used in the transient tire-force Eq. (16) to determine the contact-patch slip angle θ for each axle; i.e.

$$
\dot{\theta}_i = (\tan\theta_i - \tan\alpha_i)K_{\ell i}U_i/(dY/d\theta)_i \tag{23}
$$

where i denotes F, R, or T for the front, rear, or trailer tires, respectively.

The kinematic relations for the axle velocities U_i are as follows:

$$
\begin{aligned}
U_F &= U\cos\delta_F + (V + ra)\sin\delta_F \\
U_R &= U\cos\delta_R + (V - rb)\sin\delta_R \\
U_T &= \left[U\cos\psi + (V - rh_1)\sin\psi\right]\cos\delta_T \\
&+ \left[(V - rh_1)\cos\psi - U\sin\psi - (h_2 + c)(r + \dot{\psi})\right]\sin\delta_T
\end{aligned}
\tag{24}
$$

The aerodynamic forces are calculated as follows. The drag forces are:

$$
X_{AC} = -q_C A_C C_{DC} \tag{25}
$$

$$
X_{AT} = -q_T A_T C_{DT}
$$

where A_C and A_T denote car and trailer areas, and

$$q_C = \rho(U^2 + V^2)/2 \quad ; \quad q_T = \rho(U_T^2 + V_T^2)/2$$

$$U_T = U\cos\psi + (V - rh_1)\sin\psi$$

$$V_T = -U\sin\psi + (V - rh_1)\cos\psi - (r + \dot{\psi})h_2$$

The aerodynamic lift forces are found using:

$$Y_{AC} = -q_C A_C C_{YC} \text{ atan}(V/U)$$

$$Y_{AT} = -q_T A_T C_{YT} \text{ atan } (V_T/U_T) \quad (26)$$

These aerodynamic forces act to cause moments about the body centers of mass. These aerodynamic moments are as follows:

$$T_{AC} = q_C A_C(a + b)C_{TC} \text{ atan}(V/u)$$

$$T_{AT} = q_T A_T(h_2 + c)C_{TT} \text{ atan}(V_T/U_T) \quad (27)$$

The roll-steer compliances are determined on a quasi-static basis, and are products of the body-roll influence coefficient R (roll per unit applied lateral force at the CG) and the axle roll-steer coefficient δ_ϕ (axle steer angle per unit body roll angle). Thus

$$C_R = R_{\phi C}\delta_{\phi C} \quad ; \quad C_T = R_{\phi T}\delta_{\phi T} \quad (28)$$

The body-roll influence coefficient R can be measured, or it can be estimated from vehicle properties; δ_ϕ is best determined by measurement. We use measured data from STI [2, 10, 25, 26, 27] for R and δ_ϕ. We estimated R by taking moments about the vehicle centers of mass of the forces applied to the car trailer system during a steady-state turn. Tire forces were considered to be applied to the bodies at the axle roll centers. The values we thus estimated agreed closely with those reported by STI, and we used the latter value.

The articulation torque T_ψ represents the load-transfer device. The procedures used for modelling this device are discussed in the Load-Transfer Device Section.

EQUATIONS OF MOTION FOR 6DOF

We shall not present here the equations for our six-degree-of-freedom model 6DOF. They have not actually ever been written out by us, their formulation having been achieved by the computer completely by numerical means. The formulation technique has been described by Anderson [1].

We shall however present results obtained with 6DOF, and compare those with results obtained using 4DOF.

SOLUTION TECHNIQUES

We shall outline here, by referring to 4DOF, the techniques we employed to solve for the systems of differential equations comprising each of the two models 4DOF and 6DOF.

The system of differential equations to be solved include Eq. (19) which can be written in matrix form as

$$\left[A(\{q\},t)\right]\frac{d}{dt}\{\dot{q}\} = \{R(\{q\},\{\dot{q}\},t)\} \quad (29)$$

There is also a set of first-order differential equations to be solved. For example, there are the tire-flexibility equations Eq. (13); there is also a first-order differential equation $d\psi/dt = \dot{\psi}$ required to determine ψ from $\dot{\psi}$ in Eq. (19). Write this set of first-order differential equations as

$$\frac{d\{q\}}{dt} = \{F(\{q\},t)\} \quad (30)$$

We thus formed from Eq. (29) and Eq. (30) a system of first-order differential equations of the form

$$\frac{d}{dt}\{\dot{q}\} = \left[A\right]^{-1}\{R(\{q\},\{\dot{q}\},t)\}$$

$$\frac{d}{dt}\{q\} = \{F(\{q\},t)\} \quad (31)$$

This system of first-order equations was integrated using the conventional fourth-order Runge-Kutta method [6] with initial conditions appropriate for the conditions we were trying to simulate. The calculations were straightforward and were performed using FORTRAN programs on a Burroughs B6700 computer.

The STI data were filtered by them using an R-C filter as shown in Fig. 9 before being recorded on magnetic tape in analog form. The filter output signal S_o is related to the input signal S_i by the differential equation

$$\frac{dS_o}{dt} = (1/RC)(S_i - S_o) \quad (32)$$

We numerically integrated this differential equation simultaneously with the solution of Eq. (31) for each output variable to be compared with STI data. Thus, both filtered and unfiltered output is obtained from our simulations. The differences between the filtered and unfiltered results were approximately 10% at a maximum and generally much less than that.

RESULTS

In this section we shall present results which we obtained with each of our two models, 4DOF and 6DOF, and compare those results with experimental data obtained by STI. To validate the models we shall first present results for parameter values specified by STI as being nominal for the configurations tested. In the Sensitivity Studies Section we shall present results from a sensitivity study for 4DOF in which we varied some parameters away from their nominal values to indicate the importance of aerodynamic forces, lateral tire flexibility, the load transfer device, nonlinearities, and roll-steer compliances.

STI tested a total of 16 configurations or combinations of towing-vehicle and trailer. These tests were classified into two series, depending on the towing vehicle used. The 100 series had eight configurations, all involving a 1974 Chevrolet Nova hatchback as the towing vehicle. The 200 series had eight configurations all involving a 1973 Chevrolet Caprice station wagon as the towing vehicle. We used data for four configurations from this latter series, because it was for these configurations that STI provided sufficient values of system parameters for our simulations.

The configurations we simulated are as follows:

1. Configuration 200: The 1973 Chevrolet Caprice station wagon without a trailer.
2. Configuration 201: The 1973 Caprice with a 3400 lb "U-Haul" Trailer. This trailer was designed to employ two axles, but in this configuration only the rear-most axle was used, the trailer center of mass being thus sufficiently forward of this axle to yield good towing stability as regards the flutter type of instability. This configuration included a trailer-hitch load-transfer device.
3. Configuration 202: This configuration is identical to Configuration 201 except that it had no load-transfer device.
4. Configuration 205: This configuration was similar to Configuration 202 except that the trailer axle was located in its most forward location to position this axle closer to the trailer center of mass than it was in Configuration 202. There was no load-transfer device for Configuration 205. The intent here was to test a system marginally stable as regards the flutter type of instability.

A wide variety of tests were conducted by STI with these configurations, involving maneuvers with and without braking. We selected three types of maneuvers for our validations: step steer, lane change, and pulse steer. The vehicle proceeded at approximately constant velocity without braking for all the maneuvers selected. Our reason for selecting these maneuvers was that it was for them that the most repeatable experimental data were obtained. We thus, randomly selected single examples of each of these three types of maneuvers for each configuration.

We shall present here comparisons only for step-steer and pulse-steer maneuvers, because the results for the lane-change maneuvers do not lead to any conclusions distinct from those we can draw from the results we shall present. Anderson [1] presented results for all three maneuvers. All results are filtered as described in the Solution Techniques Section. The tire-model parameters are shown in Table 1 and the vehicle parameters are shown in Table 2.

The model-validation results for each of the four configurations considered are shown in Figs. 10–13. Consider Fig. 10, for example. Results are shown there for two maneuvers, namely step-steer and pulse-steer. The time history for the steer angle δ_F of the front wheels is shown for each maneuver. For example, for the step-steer shown at the top, the magnitude of the steer angle increases quickly to a certain value and then remains essentially constant. Below that is shown the steer-angle time history for the pulse-steer maneuver, a sharp increase to a maximum value followed by an equally fast return to approximately zero steer angle. For each of these maneuvers, results are shown for three variables, the yaw rate r, the car lateral acceleration a_y, and car roll angle ϕ. All the results for each of these variables are shown in a vertical array. For example, proceed from top to bottom in the vertical array for the yaw rate. We compare at the top, results obtained using our model 4DOF (dashed) with the STI data (solid); we show below, results from our model 6DOF (dashed) with the same STI data (solid) for the same maneuver, a step-steer. Then below that, we compare our results (dashed) first for 4DOF and then below, for 6DOF with the STI data (solid) for the pulse-steer maneuver. We have thus packed a very large amount of data into each figure.

Fig. 10 shows results for Configuration 200, the Chevrolet Caprice station wagon without a trailer. The simulation results for this configuration were obtained by assigning small values to all trailer parameters, which made the effects of the trailer negligible.

Consider the step-steer maneuver for Configuration 200 in Fig. 10. Both 4DOF and 6DOF yield excellent simulations for all the results shown. Recall that 4DOF calculates the roll ϕ on a quasi-static basis simply as being proportional to the lateral acceleration a_y, while 6DOF actually calculates the roll dynamically. Both models seem to do equally well.

Fig. 11 shows our results for Configuration 201. Consider first the step-steer maneuver. Here 4DOF and 6DOF both do equally well in predicting yaw rate r and lateral acceleration a_y. However, as regards roll angle ϕ, the predictions obtained by 6DOF are definitely superior to those for 4DOF, with both models predicting larger roll angles than reported by STI. Now consider the pulse-steer maneuver. Here the predictions for both models differ from the experimental data more than they did for the step-steer maneuver. Both models do almost equally well at predicting yaw rate and lateral acceleration, 6DOF being perhaps slightly better than 4DOF. Again 6DOF is markedly superior to 4DOF for predicting the roll angle ϕ. Recall again that 4DOF predicts the roll on a quasi-static basis whereas 6DOF actually calculated the roll dynamically.

Figs. 12 and 13 show our results for Configurations 202 and 205. Both 4DOF and 6DOF do well at predicting the yaw and the lateral acceleration for each of these configurations, with 6DOF being marginally superior. Again, however, roll behavior is predicted much better by 6DOF than it is by 4DOF. Also, the roll predictions yielded by the models are significantly less accurate than their predictions of yaw rate and lateral acceleration. Fig. 13 shows that both models do a good job of predicting the marginally stable behavior of Configuration 205.

Reviewing all the results shown in Figs. 10–13, we can say that both 4DOF and 6DOF do a good job of modelling system behavior as regards yaw rate and lateral acceleration. As regards roll, the predictions of 4DOF and 6DOF both deviate significantly from the observed behavior, with 4DOF deviating

more than 6DOF. This points out the fact that the lateral dynamic behavior of the systems considered here is only weakly dependent on roll. Therefore, for those variables which are first-order measures of lateral-dynamics behavior, such as yaw rate, r, lateral velocity V, and articulation angle ψ, there is little difference between the simulations yielded by 4DOF and 6DOF. The lateral acceleration a_y is V + rU and is thus also a first-order measure of lateral-dynamics behavior. What we have demonstrated here is that the relative inability of 4DOF to predict roll accurately is really irrelevant for this vehicle system if only lateral dynamics is of concern.

This weak coupling between roll and the lateral dynamics is due to the fact that this coupling is primarily through roll-steer effects. For the system we have considered, the only roll-steer effects occur at the rear axle of the towing vehicle. The trailer had zero roll-steer coupling, and any roll-steer effects at the front wheels of the towing vehicle were masked out by treating the actual steer-angle history of these front wheels as input data for the simulation.

Other roll-related effects which were taken into account in 6DOF, and neglected in 4DOF, pertain to effects of roll-induced changes in normal forces on the tires. Apparently such effects were truly negligible.

Note that we have not said that roll-steer effects were negligible. Recall that we used a quasi-static approach to estimate roll for 4DOF wherein we assumed the body roll to be proportional to the lateral acceleration. We shall present subsequently, results from a sensitivity study which indicates that the quasi-static approach used in 4DOF was beneficial for that simulation.

SENSITIVITY STUDIES

The object of this section is to describe tests made with the four-degree-of-freedom model (4DOF) to determine the sensitivity of this model to certain phenomena which were represented in the model. The phenomena and the tests made concerning them are as follows:

Aerodynamic forces (included and neglected)
Lateral tire flexibility (flexible tires and rigid tires)
Load-transfer device (included and neglected)
Nonlinearities (nonlinear and linearized)
Roll-steer (included and neglected)

The determination of the effects of these phenomena was straightforward with the exception of lateral tire flexibility and nonlinearities in the equations of motion. Attempts to make the tires rigid, simply by increasing the side-wall stiffness K_ℓ, introduced numerical instabilities; these instabilities were coped with by setting the tire contact-patch slip angle θ equal to the wheel-center slip angle α. The sensitivity to nonlinearities was determined using numerical linearization by running solutions with steering inputs a small fraction of the STI values, and scaling the simulation output up by a factor equal to the inverse of that fraction. Factors of 100 and 1000 were found to yield results agreeing to four significant figures, 1000 being used for the results shown here.

Typical results from these sensitivity studies are shown in Fig. 14. Yaw-rate and lateral-acceleration results are shown for each of the five phenomena considered. Anderson [1] has presented a more extensive sensitivity study, the conclusions from his study being consistent with those drawn here.

The inclusion of aerodynamic forces can be seen from Fig. 14 to have a small effect on the results yielded by the simulation. The results shown here were for a step-steer test with Configuration 202. Comparison of Fig. 12 with these results in Fig. 14 shows that the inclusion of aerodynamic forces had a small beneficial effect on the simulations. Sensitivity tests as regards aerodynamic forces were also run for pulse-steer tests, and the effects of aerodynamic forces were found to be much smaller, practically insignificant. This is consistent with the results we have shown in Fig. 14 which suggest that the primary effect of aerodynamic forces is on the steady-state vehicle behavior. In assessing the significance of these results it is important to note that the aerodynamic forces considered here are for a vehicle moving through quiesient air. Lateral gusts would be another matter, and it is well recognized that such gusts can have a significant effect on vehicle behavior [9].

The importance of lateral tire flexibility is shown in Fig. 14 for a pulse-steer test with Configuration 202. The effects are shown to be exceedingly small. Furthermore, the tire-flexibility effects on the simulation are sometimes favorable and other times adverse. There has been considerable divergence of opinion in the literature concerning the effects of lateral tire flexibility. Gough and Allbert [8] and Lippmann and Oblizajek [12] concluded that quantitative measures of such effects as regards vehicle handling characteristics are negligible, whereas Schuring and Gusakov [22] suggested that such effects could be significant. Our results indicate that tire lateral-flexibility effects on quantitative vehicle-system handling characteristics are very small indeed for the vehicle we have studied. This is consistent with the observation that the lateral forces for the tires used, build up to their steady-state values after the tires have rolled approximately one revolution.

The sensitivity of the simulation to the load-transfer device was studied by running step-steer simulations of Configuration 201 with and without the load-transfer device. There is a marked difference in the two simulations. Furthermore, comparison of the results shown in Fig. 14 with those in Fig. 11 shows that inclusion of the model of the load-transfer device in the simulation yields much better results than would be obtained by neglecting it. These results suggest that our model of the load-transfer device made an important and beneficial contribution to the quality of our simulations.

The results of our sensitivity tests as regards the effects of nonlinearities in the equations of motion yielded some surprising results. As shown in Fig. 14 for step-steer of Configuration 202, there is very little difference between the results yielded by the linear and nonlinear simulations. On the other hand, a more detailed examination of these simulations revealed that the predicted values of tire side-slip angles differed markedly for the linear and nonlinear simulations. Further examination revealed that there was, nonetheless, very little difference in the predicted values of lateral tire forces! Each simulation seemed to generate whatever tire-slip angles were necessary to generate the path of the vehicle, that path being nearly the same for the linear and nonlinear simulations. The fact that the linear and nonlinear simulations yielded results in close agreement fortunately supports the conventional technique of using linear models for investigating vehicle stability.

We conclude our sensitivity discussion with an investigation of the effects of roll steering. We compare, in Fig. 14, results obtained with our simulations for step-steer tests of Configuration 202. This test was selected because it involved a relatively high velocity and thus a relatively large amount of roll. It can be seen from Fig. 14 that there was a significant roll-steer effect, and comparison of Fig. 14 with the correspond-

ing results in Fig. 12 shows that incorporation of roll-steer effects had a favorable effect on the quality of the simulation. Thus, even on a quasi-static basis as done with 4DOF, incorporation of roll-steer effects is advantageous.

As regards the relative importance of the various effects we have discussed in this section, we would list them, with the most important listed first, as follows:

1. Load-transfer device
2. Aerodynamic forces and roll steer, equally important
3. Nonlinearities
4. Lateral tire flexibility

The order of this list is appropriate for the specific vehicle system we considered, and might not be correct for a different system.

CONCLUSIONS

Perhaps the most important conclusions to be reached are that we were able to obtain excellent simulations using models having only four and six degrees of freedom, and that the simpler model with only four degrees of freedom produced results concerning handling characteristics which were virtually as good as those for the six-degree-of-freedom model. The four-degree-of-freedom model did very well as regards all variables having an immediate bearing on handling characteristics, and did less well in predicting body roll, which has only an indirect bearing on handling characteristics through roll-steer effects. Given the relative complexity of 6DOF and the relative complexity of the data which must be supplied to it, we feel that the advantages which 6DOF offers as regards accuracy, are so marginal relative to 4DOF that we favor use of 4DOF.

The basic features of the simpler four-degree-of-freedom model have been presented by Ellis [7]. However, until now these models have remained essentially untested. We incorporated some effects which have not generally been included in car-trailer models, namely aerodynamic forces, lateral tire flexibility, a model of a load-transfer device, and roll-steer effects. All these effects contributed in a small and cumulatively beneficial way except for the model of the load-transfer device, which had a first-order beneficial effect.

The most important single contribution towards making our validation work possible was the availability of the excellent experimental data and the thorough associated documentation by Systems Technology Inc. (STI) [2, 10, 25, 26, 27]. We were the beneficiaries of being the first to be able to use these data.

The most critical aspect of our simulations definitely concerns the modelling of tire forces. Here, we were again fortunate in having available accurate empirical representations of tire-force data obtained by Calspan Corp. [3, 5, 13, 15 – 24] as described by Bohn and Keenan of Johns Hopkins Univ. [4]. Accurate representations of tire performance data are an essential ingredient in road vehicle simulations.

We believe that considerable potential exists for extending our four-degree-of-freedom model. We shall present several examples. We found that a quasi-static-equilibrium approach was useful for approximating the effects of vehicle roll on handling characteristics. This same approach could be used to approximate the effects of normal-force transfer (due to lateral accelerations) on tire-force characteristics. Our model could be extended to cover non-uniform braking and traction forces by applying appropriate combinations of a longitudinal force and a couple to each axle. We believe that 4DOF could be extended to apply to vehicles with multiple axles by the simple expedient of using a resultant force and a resultant couple to represent the total force reaction of a group of tires and axles.

We believe that our results involving the load-transfer device are especially significant. We had originally believed that the only effect of the load-transfer device as regards handling characteristics was due to change in tire-force characteristics caused by changes in normal loads on the tires. We found that such effects were exceedingly small. Re-examination of the load-transfer device then led us to model it as an articulation stiffness with stick-slip characteristics (slipping for sufficiently large variations in articulation angle). This model yielded excellent simulations, and we believe it to be a good representation of the particular load-transfer device used. Most importantly, this load transfer device has a definite beneficial effect on vehicle behavior, and we attribute this beneficial effect primarily to the articulation stiffness. This suggests that more direct methods of obtaining articulation stiffness be considered, and that studies be made to determine more extensively the effects of articulation stiffness on the handling characteristics of car-trailer systems.

To summarize, we favor simplicity. We believe that by an artful modelling process it is possible to represent the handling behavior of car-trailer systems accurately using models having only four degrees of freedom.

ACKNOWLEDGEMENTS

We would like to express our appreciation to the National Research Council and the Transportation Development Agency, both of the Government of Canada. The National Research Council supported this work through Grant A7434 and a scholarship in 1973-74 for Dr. R. J. Anderson. The Transportation Development Agency supported Dr. Anderson with a Fellowship from 1974 through 1977.

REFERENCES

1. Anderson, R. J., Dynamic Handling Characteristics of Car-Trailer Systems: Development and Validation of Mathematical Models. Ph.D. Thesis, Queen's University at Kingston, Ontario, Canada (1977).

2. Ashkenas, I. L., et al., Handling Test Procedures for Passenger Cars Pulling Trailers, Volume III: Appendices. Systems Technology Incorporated, Report No. TR-1052-1, Contract No. DOT-HS-4-00900 (January 1976).

3. Bird, K. D. and Martin, J. F., The Calspan Tire Research Facility, Design, Development and Initial Test Results. SAE Trans., Vol. 82, pg. 2012 (1973).

4. Bohn, P. F. and Keenan, R. J., Hybrid Computer Vehicle Handling Program. AOL, The Johns Hopkins University. Report No. DOT-HS-801 290 (November 1974).

5. Calspan Corp., Experimental Validation of the Calspan Tire Research Facility. Calspan Report ZM-5269-K-1 (December 1973).

6. Crandall, S. H., Engineering Analysis, McGraw-Hill Book Co., 1956.

7. Ellis, J. R., Vehicle Dynamics. Business Books, Ltd., London (1969).

8. Gough, V. E. and Allbert, B. J., Tyres and the Design of Vehicles and Roads for Safety. Proc. Auto. Div. I. Mech. E. 1968-69, Vol. 183, Pt. 3A, pp. 154-163.

9. Hucho, W. H. and Emmelmann, H. J., Theoretical Prediction of the Aerodynamic Derivatives of a Vehicle in Cross Wind Gusts. SAE Trans., Vol. 82, pg. 892 (1973).

10. Johnston, D. E., Zellner, J. W. and Ashkenas, I. L.,

Handling Test Procedures for Passenger Cars Pulling Trailers, Vol. II: Technical Report. Systems Technology Inc., Report No. TR-1052-1 (January 1976).

11. Kurtz, Jr., E. F. and Anderson, R. J., Handling Characteristics of Car-Trailer Systems; A State-of-the-Art Survey. Vehicle Systems Dynamics, June (1977), pp. 217-243.

12. Lippmann, S. A. and Oblizajek, K. L., Lateral Forces of Passenger Tires and Effects on Vehicle Response During Dynamic Steering. SAE 760033.

13. Martin, J. F., Force and Moment Characteristics of Passenger Car Tires. Calspan Corp., Report No. YD-3160-K-1 (October 1973).

14. Moore, D. F., The Friction of Pneumatic Tires. Elsevier Scientific Publishing Company, Amsterdam (1975).

15. Roland, R. D. and Rice, R. S., Tire Properties Effects on Passenger Car Handling. SAE 741108.

16. Roland, R. D., et al., The Influence of Tire Properties on Passenger Vehicle Handling. Vol. I. Summary Report. Calspan Corp., Contract No. DOT-HS-053-3-727 (January 1975).

17. Roland, R. D., et al., The Influence of Tire Properties on Passenger Vehicle Handling. Vol. II. Technical Report. Calspan Corp., Contract No. DOT-HS-053-3-727 (January 1975).

18. Roland, R. D., et al., The Influence of Tire Properties on Passenger Vehicle Handling. Vol. IV. Appendices F-H. Calspan Corp., Contract No. DOT-HS-053-3-727 (January 1975).

19. Roland, R. D., et al., The Influence of Tire Properties on Vehicle Handling. Vol. V. Measured Tire Performance Data. Calspan Corp., Contract No. DOT-HS-053-3-727 (January 1975).

20. Schuring, D. J., Rating Traction and Wear — A Review. SAE 730145.

21. Schuring, D. J., et al., The Influence of Tire Properties on Passenger Vehicle Handling. Vol. III. Appendices A-E. Calspan Corp., Contract No. DOT-HS-053-3-727 (January 1975).

22. Schuring, D. J. and Gusakov, I., Tire Transient Force and Moment Response to Simultaneous Variation of Slip Angle and Load. SAE 760032.

23. Schuring, D. J. and Roland, R. D., Radial Ply Tires — How Different are They in the Low Lateral Acceleration Regime. SAE 750404.

24. Schuring, D. J., Tapia, G. A., and Gusakov, I., Influence of Tire Design Parameters on Tire Force and Moment Characteristics. SAE 760732.

25. Zellner, J. W., Initial Tow Vehicle Data for Use in APL Simulation. Systems Technology Inc., Working Paper No. 1052-6 (April 1975).

26. Zellner, J. W., Trailer Vehicle Data for Use in APL Simulation. Systems Technology Inc., Working Paper No. 1052-8 (May 1975).

27. Zellner, J. W., Full-Scale Test Run Log, Passenger Cars Towing Trailers. Systems Technology Inc., Working Paper No. 1052-9 (November 1975).

Table 1—Tire-Model Parameters

Tire location	Front	Rear	Trailer
Tire type	H78-15	H78-15	6.70-15
Tire pressure (psig)	28	32	45
Parameters:			
A_0 (lb)	585.91	-230.1	-253.1
A_1 —	14.47	16.07	17.68
A_2 (lb)	2886	3473	3473
A_3 —	2.29	2.43	2.46
A_4 (lb)	4057	4590	4800
η —	1	1	1
B_1 (1/lb)	-2.08E-4	-1.09E-4	-1.09E-4
B_2 (1/mph)	0	0	0
B_3 —	1.216	1.216	1.216
B_4 (1/lb**2)	4.37E-9	-1.35E-8	-1.35E-8
SN —	1.0274	1.0274	1.0274
C_1 (ft/lb)	-2.52E-4	-2.06E-4	-2.06E-4
C_2 (ft/lb)	2.52E-4	1.81E-4	1.81E-4
C_3 (ft)	0	0	0
Z(200) (lb)	1441	1402	—
Z(201) (lb)	1506	1494	1550
Z(202) (lb)	1340	1703	1499
Z(205) (lb)	1416	1477	1673

Table 2—Vehicle Parameters

Configuration No.	200	201	202	205
Parameters:				
M_C (lbsec^2/ft)	176.7	176.7	176.7	176.7
M_T (lbsec^2/ft)	—	105.6	105.6	107.1
I_C (lb ft sec^2)	4289	4289	4289	4289
I_T (lb ft sec^2)	—	2356	2356	2344
a (ft)	5.14	5.14	5.14	5.14
b (ft)	5.28	5.28	5.28	5.28
c (ft)	—	1.52	1.52	0.29
h_1 (ft)	10.53	10.53	10.53	10.53
h_2 (ft)	—	11.36	11.36	9.71
$R_{\phi C}$ (rad/lb)	-2.62E-5	-3.19E-5	-3.19E-5	-3.12E-5
$R_{\phi T}$ (rad/lb)	—	0	0	0
$\delta_{\phi C}$ (rad/rad)	-0.033	-0.033	-0.033	-0.033
$\delta_{\phi T}$ (rad/rad)	—	0	0	0
A_C (ft^2)	25.1	25.1	25.1	25.1
A_T (ft^2)	—	40.52	40.52	40.52
C_{DC} —	0.564	0.564	0.564	0.564
C_{DT} —	—	0.660	0.660	0.660
C_{YC} —	-2.08	-2.88	-2.88	-2.88
C_{YT} —	—	-2.64	-2.64	-2.64
C_{TC} —	-0.63	0	0	0
C_{TT} —	—	-0.66	-0.66	-0.66
K_ψ(ft lb/rad)	—	20420	0	0
Max ($T_{\psi 1}$) (ft lb)	—	784	0	0
$T_{\psi 2}$ (ft lb)	—	605	0	0

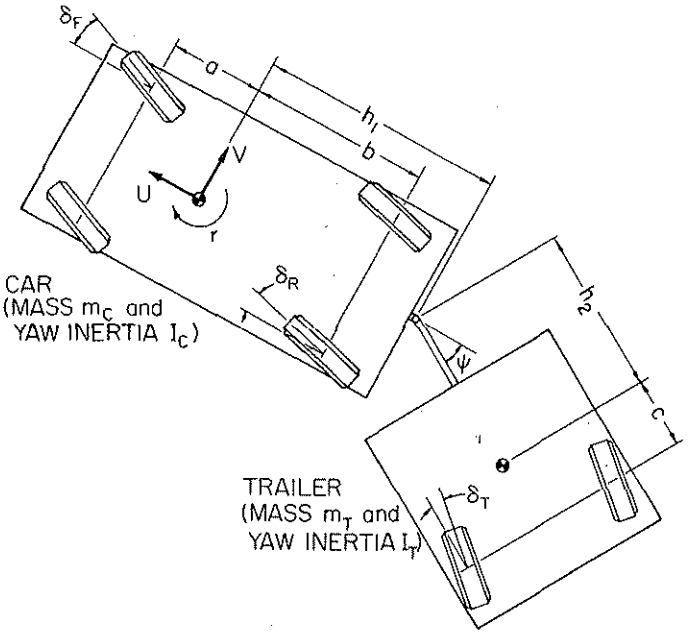

Fig. 1 — Car-trailer model with four degrees of freedom, U, V, r and ψ

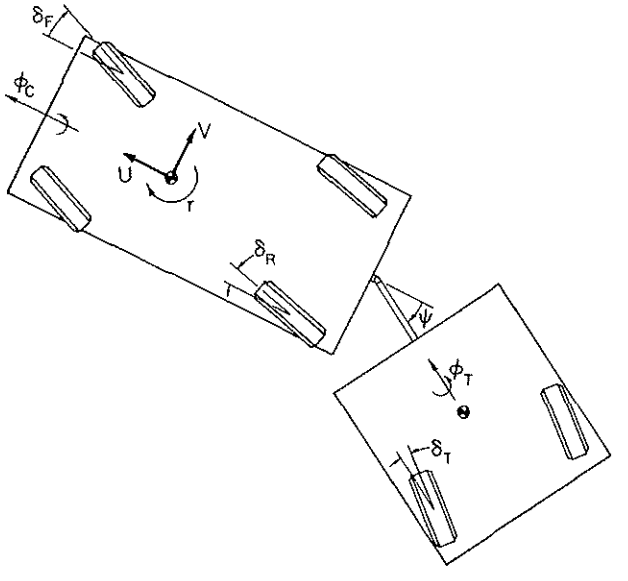

Fig. 2 — Car-trailer model with six degrees of freedom, U, V, r, ψ, ϕ_C and ϕ_T

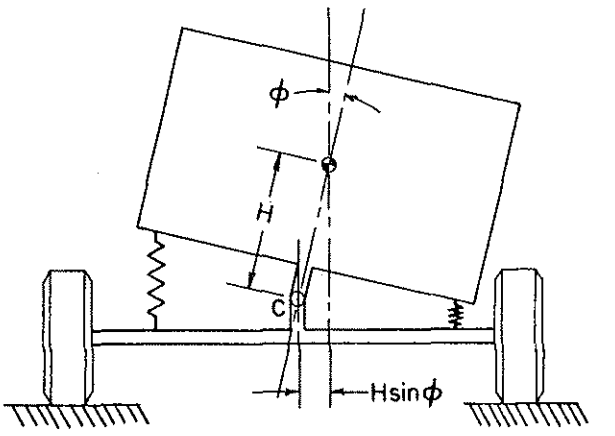

Fig. 3 — Method for estimating lateral motion of a wheel assembly due to body roll. Lateral motion of the wheel assembly is assumed equal to the lateral motion H sinϕ of the roll-center C

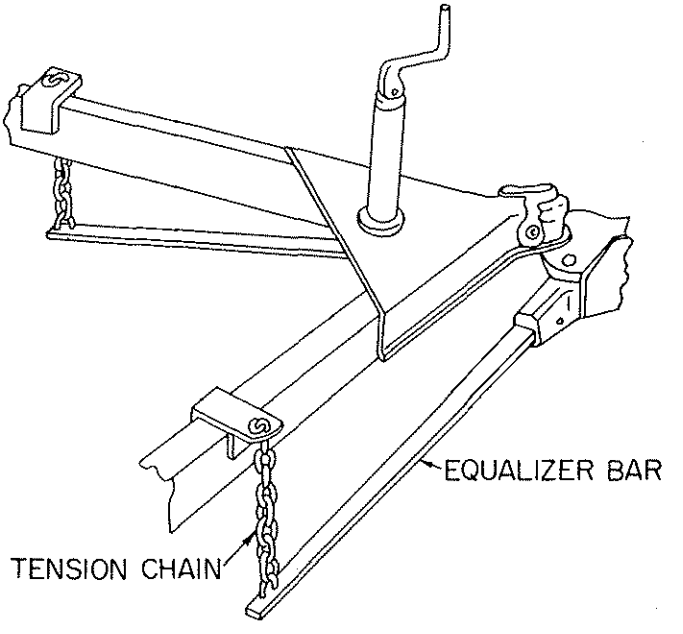

Fig. 4 — Load-transfer device. The equalizer bars are attached to the car by vertical pins which allow the bar to swing about vertical axes. The equalizer bars are attached to the trailer by tension chains

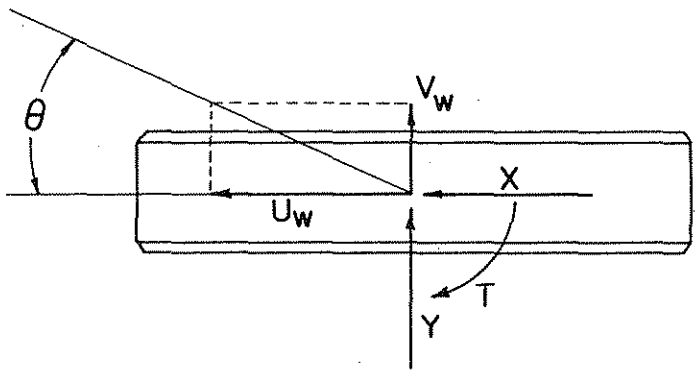

Fig. 5 — Mathematical model for representing how the articulation torque T_ψ generated by the load-transfer device depends on the articulation angle ψ

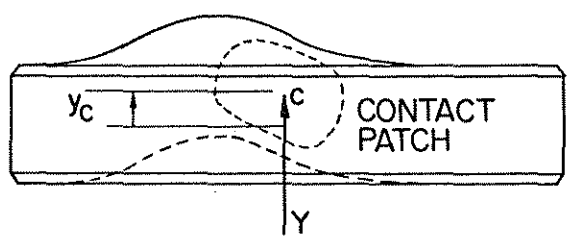

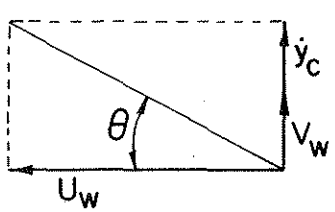

Fig. 6 — The steady-state tire contact-patch slip angle θ is defined in terms of the wheel-center velocities U_W and V_W

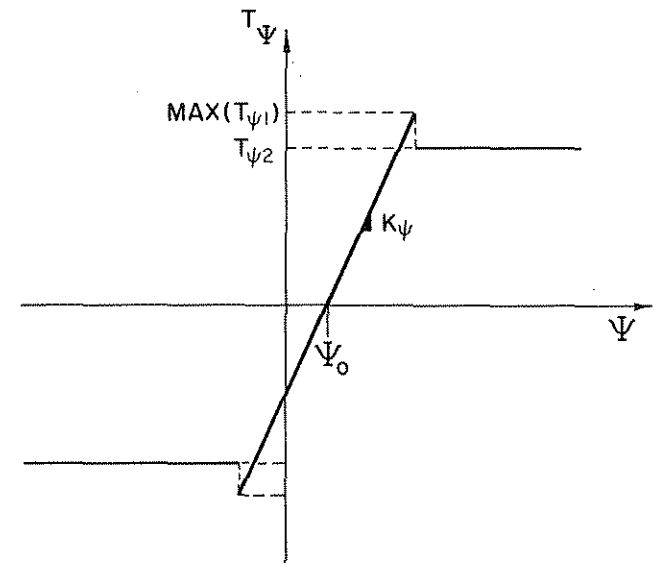

Fig. 7 — Transient tire forces were modelled simply by taking into account the effect of variations of the lateral displacement y_C of the center of the contact patch. Variations in y_C effect the slip angle θ of the contact patch

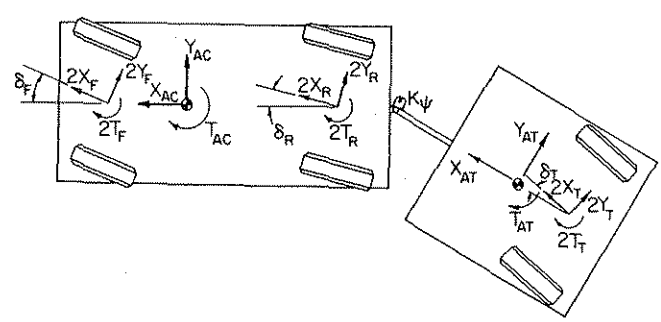

Fig. 8 — Forces exerted on the car-trailer model shown in Fig. 1

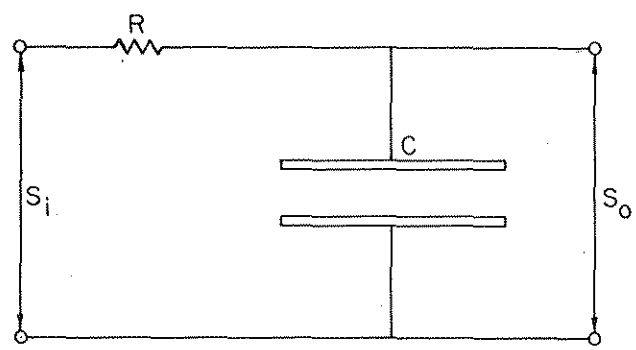

Fig. 9 — The RC filter used by STI between their transducers and their tape recorder. The time constant was RC = 20 ms

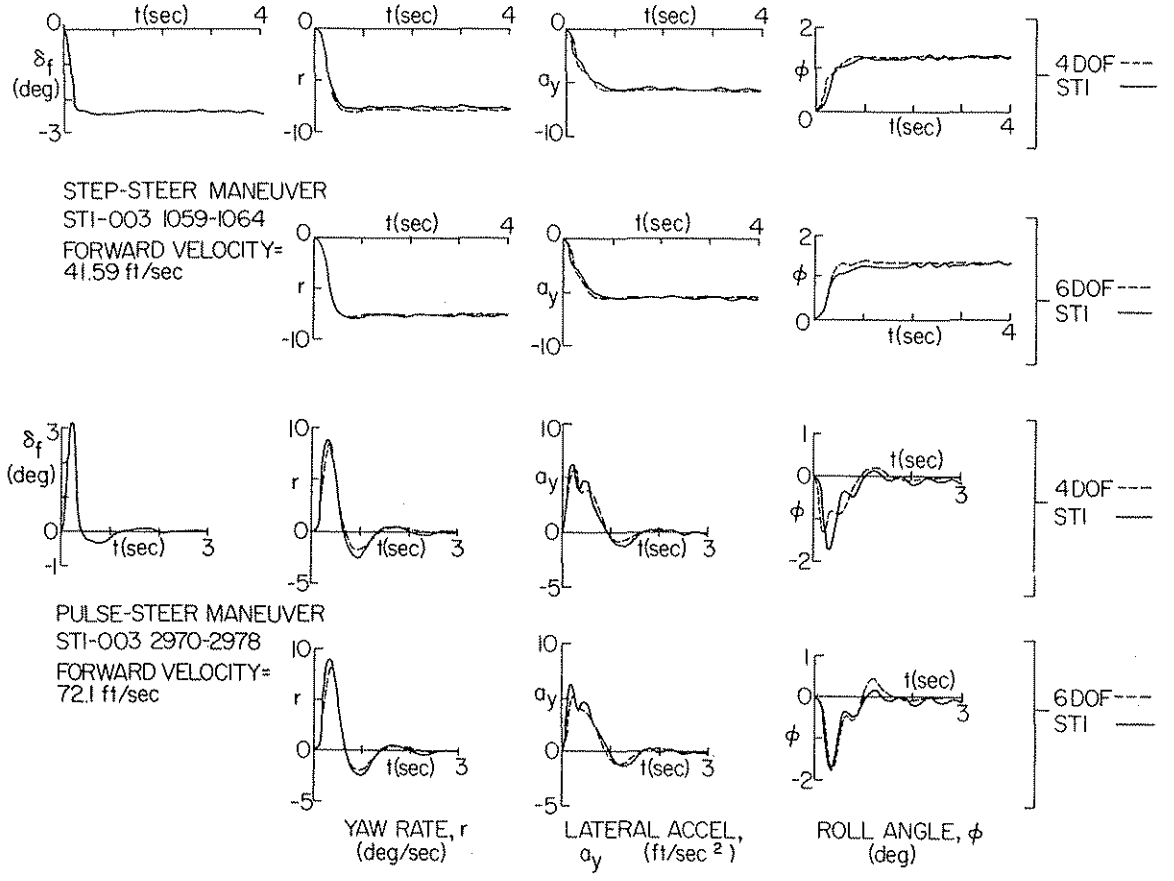

Fig. 10 — Comparison of theoretical results obtained using the models 4DOF and 6DOF with the experimental data of STI for their Configuration 200, Chevrolet Caprice station wagon without a trailer

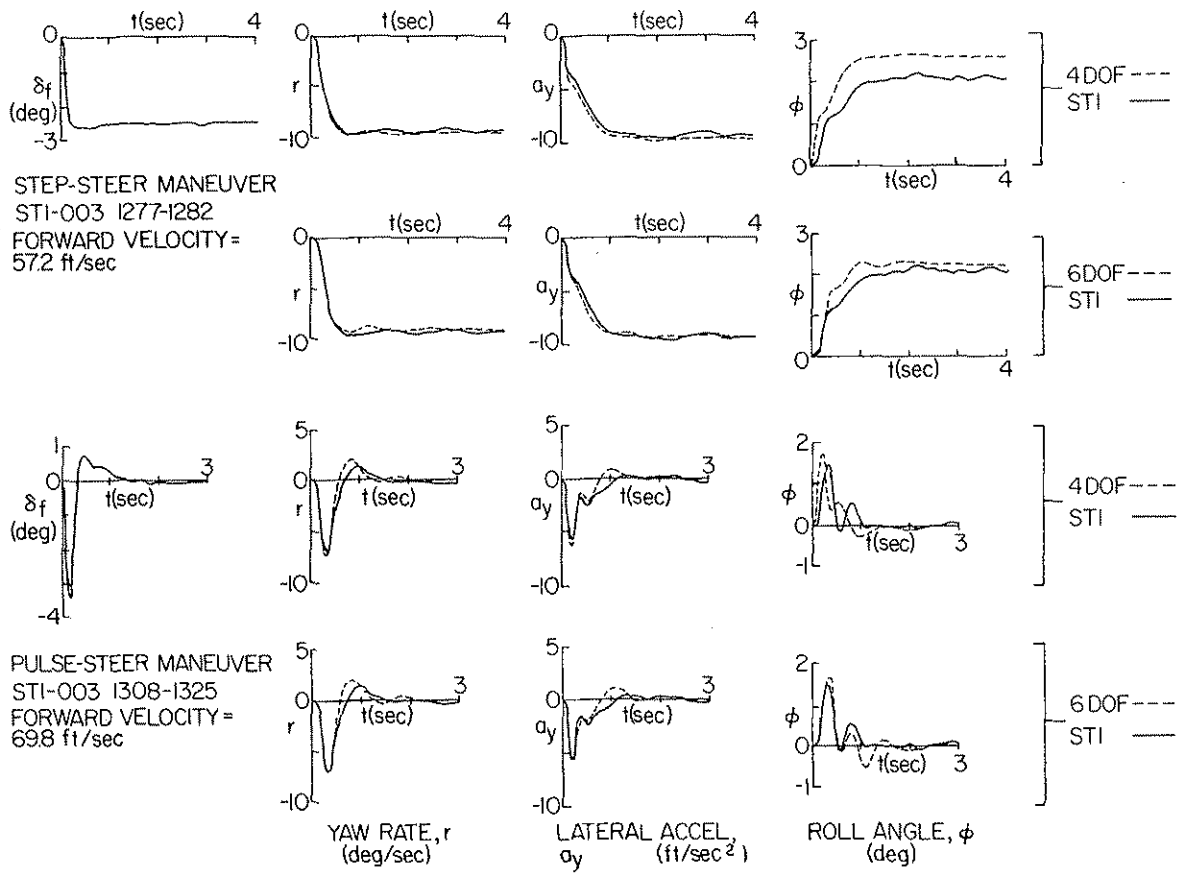

Fig. 11 — Comparison of theoretical results obtained using the models 4DOF and 6DOF with the experimental data of STI for their Configuration 201, Chevrolet Caprice station wagon with a trailer and a load-transfer device installed

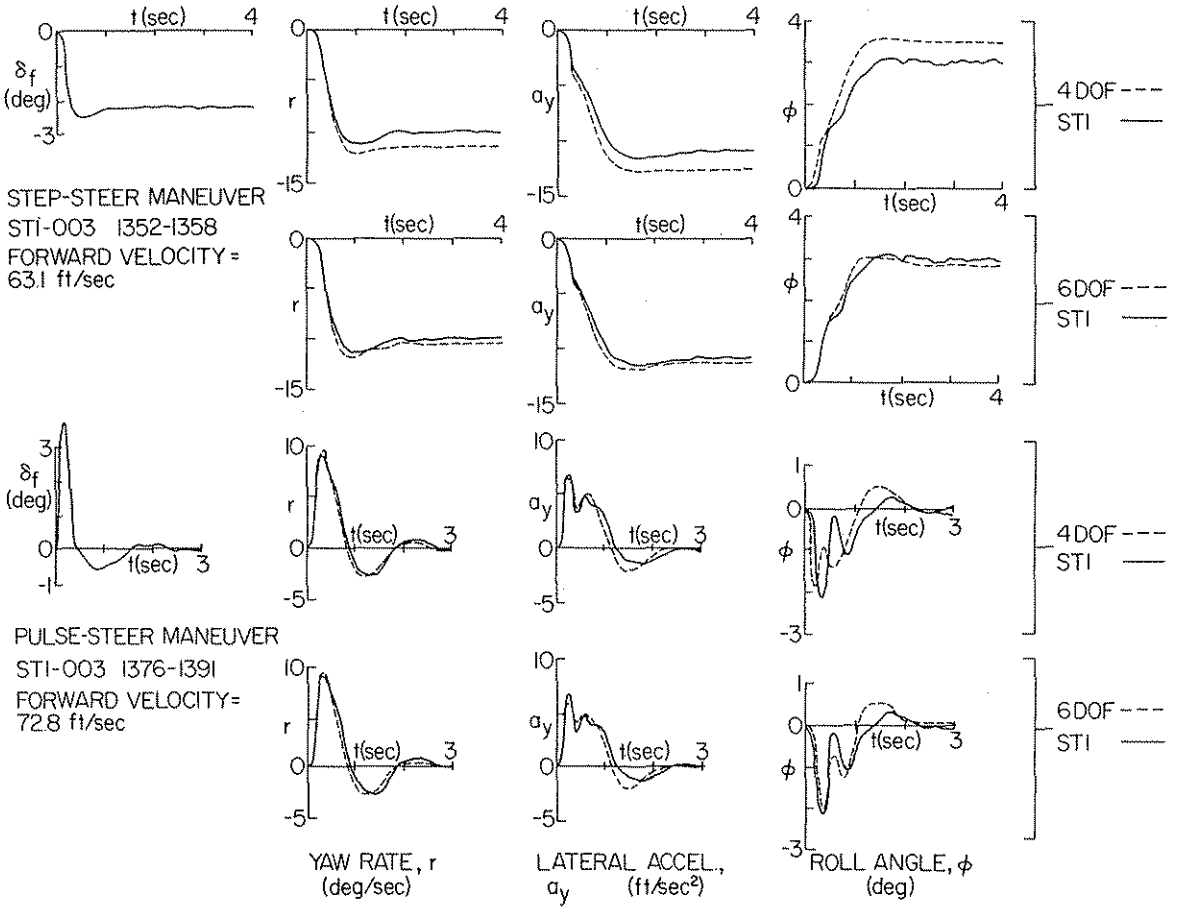

Fig. 12 — Comparison of theoretical results obtained using the models 4DOF and 6DOF with the experimental data of STI for their Configuration 202, Chevrolet Caprice station wagon with a trailer without a load-transfer device

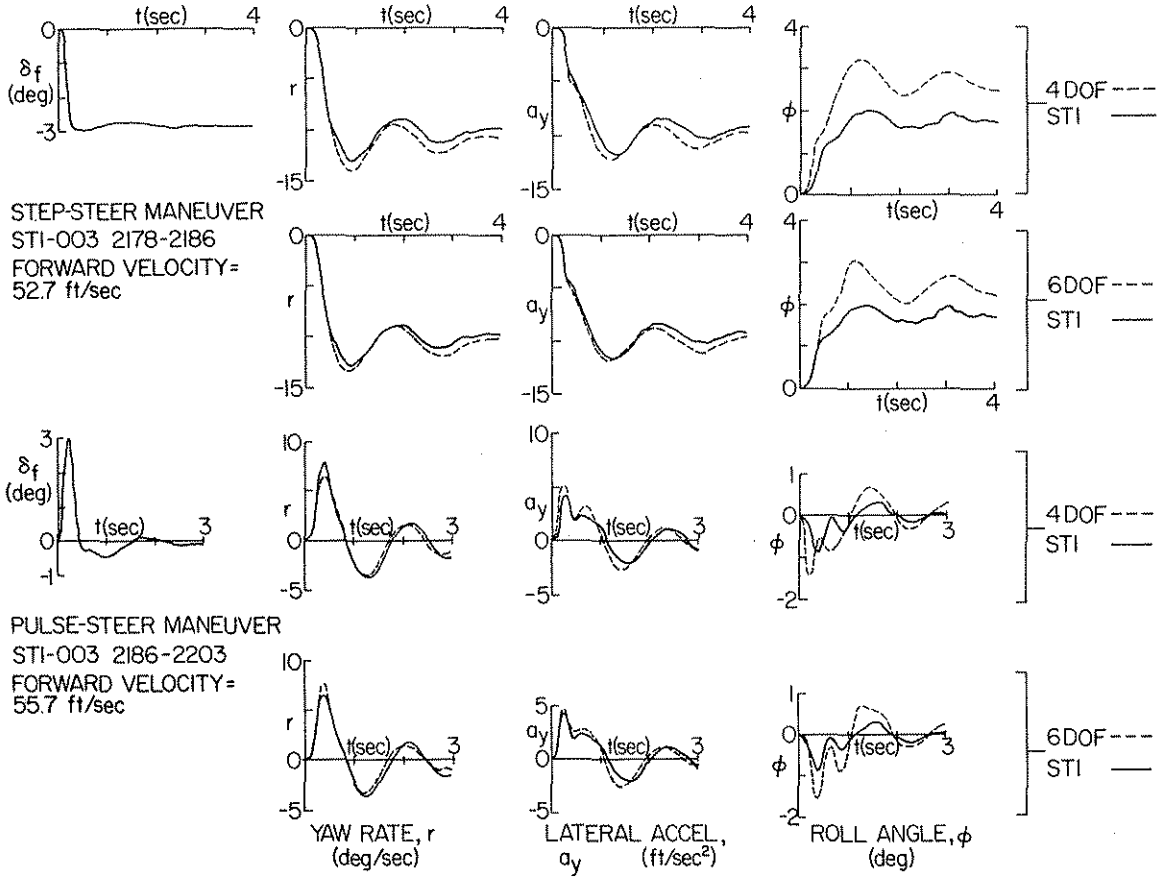

Fig. 13 — Comparison of theoretical results obtained using the models 4DOF and 6DOF with the experimental data of STI for their Configuration 205, Chevrolet Caprice station wagon with trailer without a load-transfer device and with the trailer CG close to the trailer axle to yield marginally stable behavior

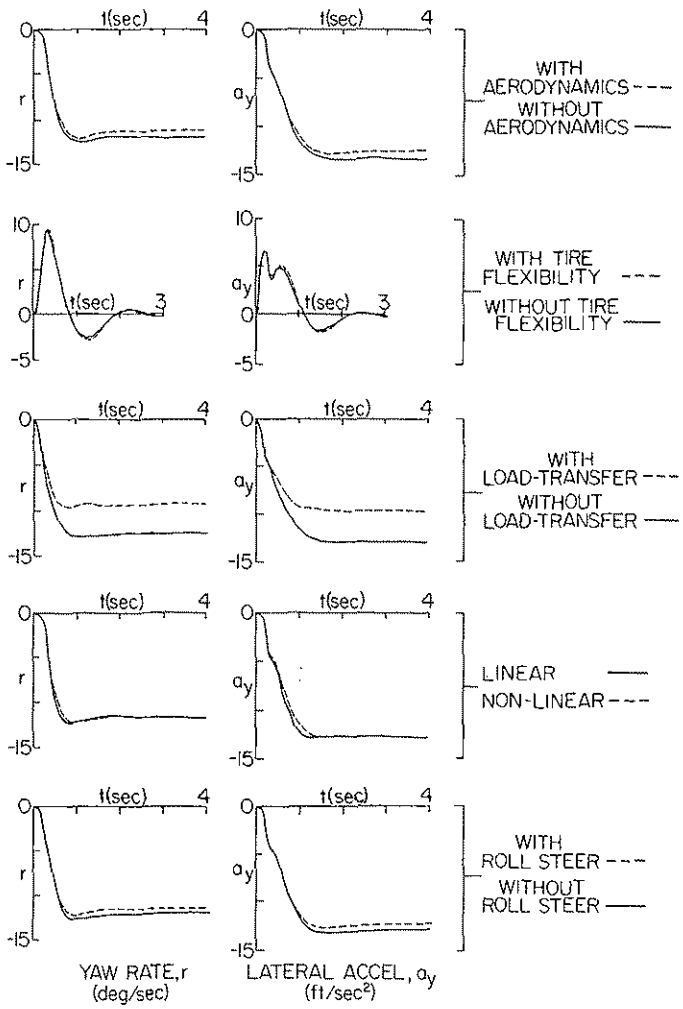

Fig. 14 — Results of the sensitivity study conducted using the model 4DOF to indicate the importance of some of the effects modelled

Society of Automotive Engineers, Inc.
400 COMMONWEALTH DRIVE, WARRENDALE, PA. 15096

104 page booklet.

Printed in U.S.A.